

12

VIRGINIA TECH CENTER FOR ADHESION SCIENCE

CAS/ESM-86-3
VPI-E-86-26

November 1986

AD-A174 832

THE DEVELOPMENT OF A MODIFIED DOUBLE CANTILEVER
BEAM SPECIMEN FOR MEASURING THE
FRACTURE ENERGY OF RUBBER TO METAL BONDS

by

D. R. Lefebvre
and
D. A. Dillard

DTIC
SELECTED
DEC 03 1986

DISTRIBUTION STATEMENT A
Approved for public release
Distribution Unlimited

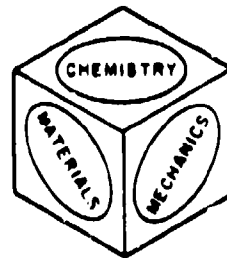
Prepared under Contract No. W00014-82-K-0185 P0005
Dr. Larry H. Peebles, Jr., Project Monitor
Office of Naval Research
Code 431
800 N. Quincy Street
Arlington, VA 22217

DTIC FILE COPY

VIRGINIA POLYTECHNIC INSTITUTE
AND STATE UNIVERSITY

218 NORRIS HALL
BLACKSBURG, VIRGINIA 24061

Telephone: (703) 961-6824
TLX: EZLINK 9103331861
VPI-BKS



86 12 02 042

REPORT DOCUMENTATION PAGE

AD-A194823

1a. REPORT SECURITY CLASSIFICATION Unclassified		1b. RESTRICTIVE MARKINGS	
2a. SECURITY CLASSIFICATION AUTHORITY		3. DISTRIBUTION/AVAILABILITY OF REPORT Distribution Unlimited	
2b. DECLASSIFICATION/DOWNGRADING SCHEDULE			
4. PERFORMING ORGANIZATION REPORT NUMBER(S) CAS/ESM-86-3 VPI-E-86-26		5. MONITORING ORGANIZATION REPORT NUMBER(S)	
6a. NAME OF PERFORMING ORGANIZATION Virginia Polytechnic Institute and State University	6b. OFFICE SYMBOL (if applicable)	7a. NAME OF MONITORING ORGANIZATION	
6c. ADDRESS (City, State, and ZIP Code) Center for Adhesion Science and Department of Engineering Science & Mechanics Blacksburg, VA 24061		7b. ADDRESS (City, State, and ZIP Code)	
8a. NAME OF FUNDING/SPONSORING ORGANIZATION Office of Naval Research	8b. OFFICE SYMBOL (if applicable)	9. PROCUREMENT INSTRUMENT IDENTIFICATION NUMBER N00014-82-K-0185 P00005	
8c. ADDRESS (City, State, and ZIP Code) 800 N. Quincy St. Arlington, VA 22217		10. SOURCE OF FUNDING NUMBERS	
		PROGRAM ELEMENT NO.	PROJECT NO.
		TASK NO.	WORK UNIT ACCESSION NO.
11. TITLE (Include Security Classification) The Development of a Modified Double Cantilever Beam Specimen for Measuring the Fracture Energy of Rubber to Metal Bonds (Unclassified)			
12. PERSONAL AUTHOR(S) Lefebvre, Didier R. and Dillard, David A.			
13a. TYPE OF REPORT Interim	13b. TIME COVERED FROM 4/85 TO 4/86	14. DATE OF REPORT (Year, Month, Day) 86/11/20	15. PAGE COUNT 27
16. SUPPLEMENTARY NOTATION Prepared for publication			
17. COSATI CODES			18. SUBJECT TERMS (Continue on reverse if necessary and identify by block number)
FIELD	GROUP	SUB-GROUP	
19. ABSTRACT (Continue on reverse if necessary and identify by block number) Rubber to metal bonds are important in a variety of automotive, tire, and marine applica- tions. A new technique is discussed for measuring the strain energy release rates of these adhesively bonded joints in the presence of harsh environments. Guidelines for design and applications are given.			
20. DISTRIBUTION/AVAILABILITY OF ABSTRACT <input checked="" type="checkbox"/> UNCLASSIFIED/UNLIMITED <input type="checkbox"/> SAME AS RPT <input type="checkbox"/> DTIC USERS		21. ABSTRACT SECURITY CLASSIFICATION	
22a. NAME OF RESPONSIBLE INDIVIDUAL		22b. TELEPHONE (Include Area Code)	22c. OFFICE SYMBOL

THE DEVELOPMENT OF A MODIFIED DOUBLE CANTILEVER
BEAM SPECIMEN FOR MEASURING THE
FRACTURE ENERGY OF RUBBER TO METAL BONDS

D. R. Lefebvre and D. A. Dillard

ABSTRACT

Rubber to metal bonds are important in a variety of automotive, tire, and marine applications. A new technique is discussed for measuring the strain energy release rates of these adhesively bonded joints in the presence of harsh environments. Guidelines for design and applications are given.

INTRODUCTION

Elastomer to metal bonding is an important adhesion problem for a variety of modern structures and components. Major applications include the automotive, tire, shipbuilding, and off shore drilling industries. In these applications, the rubber may serve to inhibit corrosion, to seal the component from intrusion of unwanted substances, or as a load bearing structure. Although acceptable bonds are routinely produced for many of these functions, bond durability can be a problem under certain environmental exposure. Of current concern are the rubber to metal bonds for marine applications. Although these bonds have been shown to

D. R. Lefebvre is Graduate Research Assistant and D. A. Dillard is Assistant Professor, Engineering Science and Mechanics Dept., Virginia Polytechnic Institute and State University, Blacksburg, VA 24061-4899.



A-1

<input checked="" type="checkbox"/>
<input type="checkbox"/>
<input type="checkbox"/>
Codes
/or
al

be quite durable in seawater environments [1], the presence of small amounts of cathodic potential can rapidly deteriorate the adhesive bond. Cathodic potential may be provided by the galvanic action of dissimilar metals. This situation is intentionally created on many marine structures by the use of sacrificial zinc anodes. Ironically, these anodes serve to protect the steel hull but degrade the performance of rubber bonds, paint, and other organic coatings. Even if the metal substrates are initially electrically insulated from the anodes, corrosion products and sediment can build up on the components to permit the flow of electrons.

Cathodic debonding processes have been widely studied by researchers in the area of thin organic coatings [2-4]. When metallic substrates are exposed to aqueous salt solutions and supplied with free electrons, reduction of dissolved oxygen or water at the adhesive to metal oxide interface occurs and locally increases the pH. When these reaction products are sequestered inside a small debonded region or adhesive layer, an extremely high pH can result. Several mechanisms have been proposed to explain the relatively rapid debonding that results from the alkaline environment [2-5]. Although the mechanisms responsible for the bond deterioration are complex and not entirely understood, our observations have indicated that the high pH hydrolyzes the polymeric primer leaving a weakened bond. The weakened zone may remain intact unless a sufficient force is applied. The objective of the current work has been to develop tests to measure the critical strain energy release rates for the rubber to metal bonds in various stages of deterioration. This paper describes a modified test for

determining G_c for elastomer to rigid adherend bonds subjected to aqueous environments.

A variety of tests have been advocated for evaluating the adhesion of a flexible layer bonded to a rigid substrate. The cone test (ASTM D-429) has been widely used for measuring the adhesion of rubber to metal substrates. The design of this test causes debonding to initiate at the interior of the specimen, however, making it inappropriate for tests subjected to environmental exposure. A number of different specimens have been based around the peel concept. These include the climbing drum peel test (ASTM D-1781), the floating roller peel test (ASTM D-3167), and the simple peel test, using 180° peel (ASTM D-903) or other angles. Unfortunately, most of these tests are quite cumbersome to use in a harsh liquid environment. In an effort to avoid some of the problems associated with these specimens for our application, several improved techniques are being developed and one of these will be reported herein.

THE DOUBLE CANTILEVER SANDWICH BEAM

The various peel tests have been utilized for measuring fracture energies of rubber to metal bonds, but they have a number of limitations. All of these tests tend to induce very large deformations at the debond tips. These extreme distortions produce significant material and geometric nonlinearities which make the specimens very difficult to analyze. If one wishes to measure time dependent fracture energies, the viscoelastic dissipation in the relatively large rubber bulk can alter the results. Although fabric can be embedded in the rubber to minimize the strain energy stored [6], localized large

deformations can still induce substantial energy dissipation in a nonlinear viscoelastic material. To minimize these difficulties, a specimen is needed in which the deformations are smaller and in which the viscoelastic dissipation is reduced.

The double cantilever sandwich beam (DCSB) illustrated in Fig. 1 is a modification of the double cantilever beam (DCB) originally proposed by Ripling, et al. [7]. The specimen is shown with an extensometer mounted on the unit for measuring the displacements during the calibration study. The specimen consists of a very thin layer of the elastomer bonded between two metal adherends. The specimen offers the ability to measure the fracture energies of elastomers bonded to relatively rigid substrates. The deformations in the elastomer are quite small, the specimen may be easily analyzed with numerical procedures or with a closed form beam on elastic foundation solution described herein, and the specimen may be tested in harsh liquid environments with simple loading fixtures. Viscoelastic dissipation is greatly reduced for three reasons: 1) the volume of the elastomer is minimal, 2) the strain levels are smaller than in other specimens, thereby minimizing the nonlinear effects, and 3) the elastomer is highly constrained, forcing it to deform in a bulk rather than shear mode. The bulk behavior of polymers tends to be substantially less time dependent than the shear behavior.

DESIGN AND ANALYSIS OF THE DOUBLE CANTILEVER SANDWICH BEAM

The experimental phase of the work was conducted on two different specimen geometries with dimensions given in Table I. Type #2 is a refined version of type #1, having thicker adherends and a thinner layer

of rubber. The steel adherends were vapor degreased, grit blasted with steel grit, and vapor degreased again in tri-chloroethane 1,1,1 in preparation for bonding. Two coats of Chemlok 205 primer (manufactured and courteously supplied by the Lord Corp.) and two coats of Chemlok 220 topcoat were brushed on the adherends, allowing each layer to dry prior to applying the next. After preheating the mold in a platen press, specimens along with uncured 5109 S Neoprene rubber were inserted. The adhesive and rubber were vulcanized at 154°C (310°F) for 1.5 hr at a nominal pressure of 3.45 MPa (500 psi).

In order to characterize the toughness of adhesive bonds, the relationship between the strain energy release rate, load, and crack length must be known. This relationship has been predicted analytically and determined experimentally. Using an MTS servo-hydraulic load frame, load-deflection behavior was obtained for the two specimen configurations as a function of crack length. Deflections were measured with an extensometer and increments in crack length were made by using a saw to cut the rubber. Although tension specimens of the rubber had exhibited considerable creep, the DCSB specimens did not show measurable time dependence, presumably because of the minimal amount of rubber loaded in a triaxial fashion.

Figure 2 illustrates the measured compliance of the type #1 specimen. The dashed line represents the predicted compliance based on neglecting the deformations in the rubber. It is the simple cantilever beam solution commonly used for the DCB specimen and assumes that the beam rests on a rigid foundation. The compliance is based on the following relationship:

$$C = 8a^3 / (Ebh^3) \quad (1)$$

where a - crack length, E - Young's Modulus of adherend, b - specimen width, and h - thickness of adherend. The measured compliance is consistently higher than the simple prediction and requires an improved approximation. To achieve this, the thin rubber layer was assumed to act as a classical elastic foundation and a closed form solution based on the finite length beam on an elastic foundation solution given by Hetenyi [8] was developed. Kanninen [9] has employed a similar beam on elastic foundation solution for the monolithic double cantilever beam specimen to account for transverse deformations.

Referring to Fig. 3, one can calculate the total beam deflection at B as:

$$y_B = y_A + \theta_A \cdot a + Pa^3/3EI \quad (2)$$

The slope and deflection at point A can be calculated by utilizing Hetenyi's solution for a finite beam on an elastic foundation. For the case of equal applied forces on the two beams, symmetry requires that there be no horizontal (frictional) forces and the fracture mode is pure mode I.

To proceed, the applied force P at point B is translated to point A and an equivalent moment is also applied at point A. The characteristic root of the governing differential equation for a beam on an elastic foundation is:

$$\lambda = \sqrt[4]{\frac{k}{4EI}} \quad (3)$$

For beams of finite length, the solution depends on the nondimensional quantity $[\lambda(L-a)]$. For the current problem, this quantity exceeds π and

according to Hetenyi, the beam may be classified as a long finite length beam. For an applied force of P at point A, the slope and deflection at A are given by:

$$\theta_A = \frac{2P\lambda^2}{k} \frac{\sinh^2 \lambda \rho + \sin^2 \lambda \rho}{\sinh^2 \lambda \rho - \sin^2 \lambda \rho} \quad (4a)$$

$$y_A = \frac{2P\lambda}{k} \frac{\sin \lambda \rho \cosh \lambda \rho - \sinh \lambda \rho \cos \lambda \rho}{\sinh^2 \lambda \rho - \sin^2 \lambda \rho} \quad \text{with: } (\rho=L-a) \quad (4b)$$

and for an applied moment of (Pa) at point A, the slope and deflection are given by:

$$\theta_A = \frac{4Pa\lambda^3}{k} \frac{\sinh \lambda \rho \cosh \lambda \rho + \sin \lambda \rho \cos \lambda \rho}{\sinh^2 \lambda \rho - \sin^2 \lambda \rho} \quad (4c)$$

$$y_A = \frac{2Pa\lambda^2}{k} \frac{\sinh^2 \lambda \rho + \sin^2 \lambda \rho}{\sinh^2 \lambda \rho - \sin^2 \lambda \rho} \quad \text{with: } (\rho=L-a) \quad (4d)$$

By superimposing these results and substituting them into Eqn. 2, one obtains a closed form solution for the deflection of the DCSB specimen.

The remaining task for completing the analysis is the determination of the foundation stiffness, k. This is a difficult parameter to determine analytically because of the complex triaxial stress state in the rubber. As a first step, k was determined from experimental compliance data. Although the calculated values of foundation stiffness show a slight decrease as the debond increases in length, the values are relatively stable and good agreement with experimental data is achieved as illustrated in Fig. 2. Again one should note, however, that the

value of k is chosen to give the best agreement with the compliance data rather than being determined independently. At this stage the foundation stiffness may be viewed as a curve fitting parameter. If one takes the observed foundation stiffness and multiplies by the thickness of the rubber layer and divides by the width of the beam, an effective elastic modulus of the rubber layer is determined. Values obtained are presented in Table II and as would be expected, due to the triaxial constraint, the effective modulus of the rubber is strongly affected by the thickness of the rubber layer. The measured values of effective modulus lie between the tensile modulus of the rubber, 4.14 MPa (600 psi), and the bulk modulus, 876 MPa (127 ksi), and increase rapidly as the rubber thickness decreases.

As a second step in ascertaining the foundation characteristics, it was shown that the foundation stiffness can be predicted analytically using a procedure developed by A.N. Gent et al. [10,11]. The overall deformation of the block of rubber is assumed to result from the superposition of the deformation of the unconstrained block and a shear deformation necessary to restore displacement continuity along the banded interfaces. The normal force may be written in the form:

$$F = f_c AE' \epsilon \quad (5a)$$

in which A is the cross-sectional area of the block, E' is Young's modulus of the rubber, ϵ is the normal strain in the rubber and f_c is a corrective factor accounting for the constraining effect of the adherends. In the case of a rectangular block of infinite length,

$A=bt$, $\epsilon = \frac{2y}{t}$ and $f_c = \frac{4}{3} + \frac{1}{3} b^2/t^2$ with b = block width, t = block thickness, y = deflection in each beam.

Whence, for a foundation of unit width the normal stress would be:

$$\sigma = f_c E' \epsilon t \quad (5b)$$

or

$$\sigma = 2f_c E' y \quad (5c)$$

Now in the theory of Beams on Elastic Foundation, the foundation stiffness k is defined by:

$$\sigma = k y/b \quad (5d)$$

Taking $b=1$ and comparing (5c) and (5d) yields:

$$k = 2f_c E' \quad (5e)$$

Table II shows that the foundation stiffness obtained from the above relationship and obtained previously by curve fitting the experimental data are in reasonable agreement. It should be noted that the solution to the deflection equation is quite insensitive to the value of k used and that excellent agreement with the experimental compliance data with variations of k as large as 30%.

It must be noted that the solution given by Gent for the infinitely long block of finite width is not completely appropriate for the solution to the beam on elastic foundation because it: 1) does not account for the end occurring at the debond tip and 2) it does not

account for the damped sinusoidal displacements. Both of these factors should result in an overprediction of the foundation stiffness. Nonetheless, the errors introduced do not seem to strongly affect the calculations of the strain energy release rate and these approximations seem adequate to estimate the foundation stiffness.

To further verify the model, a strain gage was mounted on the outer surface of one of the steel adherends and the strain was recorded for various debond distances. The results from this are presented in Fig. 4. The gage was positioned 127 mm (5 in) from the loading end. When the debond tip is near the end B, the strains measured are very small. As the debond approaches the gage, the strains go positive where the beam oscillations induce a tensile mode in the rubber. As the oscillation passes on ahead of the gage, the compressive strains induced by bending in the adherends increase up to a maximum value equal to that predicted by simple beam theory for $M = (P \cdot 127 \text{ mm})$. The predicted values of strain are seen to agree very well with the experimental data.

To better understand how various parameters affect the performance of the DCSB, parametric deflection studies are presented in Figs. 5, 6, and 7. Figure 5 illustrates the effect of the debond length on the normalized deflections for the type #1 specimen. When one considers the actual G values obtainable, they are seen to increase as the debond length increases. Figure 6 shows how changing the rubber thickness would change the deflections for a given adherend thickness. Decreasing the thickness reduces the amount of bending oscillation and shortens the characteristic oscillation distance, in addition to reducing the time dependence as mentioned before. Clearly the rubber sandwich should be made as thin as practical. Figure 7 shows that increasing the adherend

thickness dramatically reduces the oscillations in addition to increasing the maximum available strain energy for debond propagation.

In order to test loaded specimens in a harsh environment, it is highly desirable to use a simple, self-loading device. The Boeing wedge specimen is a form of the DCB and it is loaded by driving a wedge between the adherends to produce a constant displacement test. Unfortunately, the available G for this type of load is highly dependent on the debond distance, obeying an inverse fourth power relationship with a . Although this type of loading can be utilized, the technique is very sensitive to small errors in debond measurement, and the applied G decreases so rapidly that the measurements must be taken at very small increments in debonding to obtain accurate information. In an effort to avoid these difficulties, a loading device which would impose a relatively constant value of G would be beneficial.

To investigate a constant G test, one can write a closed form solution for the required force necessary to produce a constant G rate:

$$P = \frac{2Gb}{aC/aa} \quad (6)$$

The expression for aC/aa is given in Appendix A. Figure 8 represents parametric iso- G curves for specimen type #2. The indicated fracture energies are typical of G_c for the weakened bonds. The vertical portion of the limit of validity domain represents a detached length of 216 mm (8.5 in) after which the remaining support is too short for the analysis to be valid. The curved portion of the limiting domain represents rotations of the loaded end of the beam which exceed 8 degrees and may result in beam foreshortening errors.

Iso-G loading can be accomplished quite simply by using a spring to load the specimen. Figure 9 illustrates the loaded fixture in place in the testing environment. Simple helical compression springs were used to provide the energy to the system. Figure 10 illustrates the force available from a given spring for several different preload rates superimposed on a desired Iso-G curve. By properly selecting the spring stiffness and the preload, one can obtain an Iso-G test window with a width of 50 mm (2 in). Thus one is able to set up the loading device to provide a relatively constant debond driving force over a relatively long debond distance. With a small assortment of springs and with judicious choices of the preload, one can follow a required G curve over most of the length of the specimen. A compact load cell and an extensometer can be utilized to monitor the actual applied G to correct for small deviations. By holding G relatively constant, however, the collection of debond growth data is greatly simplified.

DIFFICULTIES WITH INTERACTION BETWEEN DIFFUSION AND FRACTURE

Because the specimen was designed to measure the fracture energy of debonding under conditions of cathodic delamination, the adherends were not thick enough to permit testing of the dry bond. Preliminary tests were conducted in seawater or NaOH solutions with cathodic potential applied. Slow debond rates were measured but difficulties were encountered because the results did not seem consistent. When specimens were broken open after testing, a significant chevron or reverse tunneling effect was noted. The reasons for this phenomena which is opposite of that experienced in standard DCB specimens is that the peel stresses are higher at the outside of the specimen because of the "poker

chip" effect, and because diffusion occurs from these edges into the specimen. Because the chevron effect was so severe, meaningful debond distances could not be obtained.

As other tests on the neoprene to steel bond were conducted, it became apparent that moisture diffused into the specimen and left the bond intact but severely weakened. When choosing between adhesive systems for applications exposed to cathodic potential, the two most important parameters to measure appear to be the rate at which diffusion occurs and the retained strength of the weakened bond. Although the DCSB appeared to be limited for measuring fracture parameters while diffusion into the specimen was occurring, it was decided that the important fracture parameter to measure was the critical strain energy release rate of the weakened bond. Several specimens were conditioned in environment to produce a weakened, but intact, cathodically degraded bond. By imposing potential to only one adherend, this bond was preferentially weakened. Once the specimens were conditioned, they were tested in a tension test machine. The results were repeatable and this approach seems to work quite well.

DESIGN GUIDELINES

In designing DCSB specimens, the following guidelines may prove helpful:

- * Make the thickness of the soft layer as small as practical to minimize the viscoelastic effects.
- * Select a specimen width which is large compared to the elastomer thickness in order to increase the constraining action on the elastomer.

- * Determine the appropriate G range for the adhesive system and select a beam thickness which can provide the desired G values while remaining in the small deflection envelope.
- * The remaining bonded length should be large enough that the long finite length beam assumption is valid.
- * For the Iso-G loading, superimpose the spring load decay curves on the Iso-G parametric curves and select an appropriate initial load and spring constant to give the desired result.

SUMMARY

The DCSB offers distinct advantages over other specimens for measuring the critical strain energy release rate for elastomers bonded to a rigid adherend because it minimizes the viscoelastic dissipation. It is easily fabricated and can be analyzed with a closed form beam on elastic foundation solution. Foundation stiffness can be predicted with a rubber elasticity analysis. A simple spring loading device can be used to provide near constant G loading over a relatively wide test window. When using the specimen in an environment, diffusion coming in from the sides can cause spurious results. For these cases however, specimens conditioned to equilibrium can be tested with good results.

ACKNOWLEDGEMENTS

The authors are grateful to the Office of Naval Research and the Naval Research Laboratory - Underwater Sound Reference Detachment for the support of this work. The graduate student was supported on contract #N00014-82-K-0185, and the other costs were supported by #N00014-85-K-0145.

REFERENCES

1. Stevenson, A, "On the Durability of Rubber/Metal Bonds in Seawater," International Journal of Adhesion and Adhesives, V5, N2, April 1985, pp 81-91.
2. Leidheiser, H, W Wang and L Igetoft, "The Mechanism for the Cathodic Delamination of Organic Coatings from a Metal Surface," Progress in Organic Coatings, V 11, 1983, pp 19-40.
3. Wang, W and H. Leidheiser, "A Model for the Quantitative Interpretation of Cathodic Delamination," Pourbaix Symposium Volume of the Electrochemical Society, New Orleans, October 1984.
4. Koehler, E L, "The Mechanism of Cathodic Disbondment of Protective Organic Coatings - Aqueous Displacement at Elevated pH," Corrosion - NACE, V 40, N 1, January 1984, pp 5-8.
5. Hammond, J S, J W Holubka and R A Dickie, Journal of Coatings Technology, V 51, 1979 p 45.
6. Gent, A N, "Peel Mechanics for an Elastic-Plastic Adherend," Journal of Applied Polymer Science, V 21, 1977, pp 2817-2831.
7. Ripling, E J, S Mostovoy and R L Patrick, Material Res. Stud., V 4, 1977, p 129.
8. Hetenyi, H, "Beam on Elastic Foundation," Ann Arbor, The University of Michigan Press.
9. Kanninen, M F, "An Augmented DCB Model for Studying Crack Propagation and Arrest," International Journal of Fracture, V 9, N 1, March 1973.
10. Gent, A N and E A Meinecke, "Compression, Bending, and Shear of Bonded Rubber Blocks," Polymer Engineering and Science, V 10, N 1, Jan. 1970.
11. Gent, A N, R L Henry and M L Roxburg, "Interfacial Stresses for Bonded Rubber Blocks in Compression and Shear," Journal of Applied Mechanics, Dec. 1974, p. 855.

**Table I
Specimen Dimensions**

Specimen Type	Bond Thickness	Beam Length	Adherend Thickness	Beam Width
#1	1.27 mm (0.05 in)	273 mm (10.75 in)	3.18 mm (0.125 in)	25.4 mm (1.00 in)
#2	0.76 mm (0.03 in)	267 mm (10.5 in)	6.35 mm (0.250 in)	25.4 mm (1.00 in)

**Table II
Foundation Stiffness and Effective Modulus of the Rubber Layer**

Specimen Type	Bond Thickness	Foundation Stiffness $k=2f_c E$ (Predicted)	Foundation Stiffness k (Experimental)	Effective Modulus kh/b (Experimental)
#1	1.27 mm (0.05 in)	1.11 MPa (162 ksi)	0.68 MPa (98.9 ksi)	34.4 MPa (5.00 ksi)
#2	0.76 mm (0.03 in)	3.07 GPa (446 ksi)	3.45 MPa (500 ksi)	103.5 MPa (15.0 ksi)

APPENDIX A

The compliance of a DCSB specimen is given by: $C = 2y_B/P$

$$C = \frac{1}{EI\lambda^3} \frac{\sinh\lambda\rho \cosh\lambda\rho - \sin\lambda\rho \cos\lambda\rho}{(\sinh^2\lambda\rho - \sin^2\lambda\rho)} + \frac{a}{EI\lambda^2} \frac{\sinh^2\lambda\rho + \sin^2\lambda\rho}{(\sinh^2\lambda\rho - \sin^2\lambda\rho)}$$

$$+ \frac{2a^2}{EI\lambda} \frac{\sinh\lambda\rho \cosh\lambda\rho + \sin\lambda\rho \cos\lambda\rho}{(\sinh^2\lambda\rho - \sin^2\lambda\rho)} + \frac{2a^3}{3EI} (g)$$

where: $\rho = (L-a)$

The derivative of the compliance with respect to debond length is given by:

$$dC/da = \lambda \frac{JC}{JD} \quad \text{with } D = \lambda(L-a)$$

$$\frac{JC}{JD} = \frac{1}{EI\lambda^3} \frac{(\cosh^2 D + \sinh^2 D - \cos^2 D + \sin^2 D)(\sinh^2 D - \sin^2 D) - 2(\sinh D \cosh D - \sin D \cos D)^2}{(\sinh^2 D - \sin^2 D)^2}$$

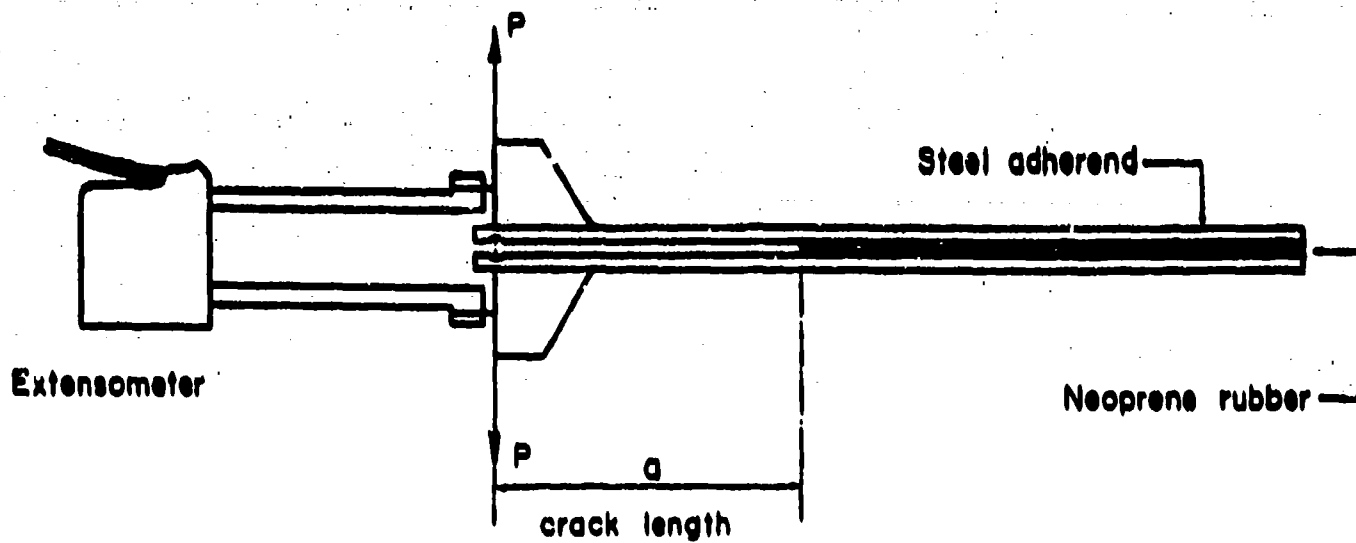
$$+ \frac{2}{EI\lambda^2} \{ [2(\sinh D \cosh D + \sin D \cos D)(L-D/\lambda) - 1/\lambda(\sinh^2 D + \sin^2 D)] (\sinh^2 D - \sin^2 D) \}$$

$$- 2(\sinh^2 D + \sin^2 D)(L-D/\lambda)(\sinh D \cosh D - \sin D \cos D) \} / (\sinh^2 D - \sin^2 D)^2$$

$$+ \frac{2}{EI\lambda^2} \{ [(\cosh^2 D + \sinh^2 D + \cos^2 D - \sin^2 D)(L-D/\lambda^2) - 2/\lambda(L-D/\lambda)(\sinh D \cosh D + \sin D \cos D)] \}$$

$$\times (\sinh^2 D - \sin^2 D) - 2(L-D/\lambda)^2 (\sinh^2 D \cosh^2 D - \sin^2 D \cos^2 D) \} / (\sinh^2 D - \sin^2 D)^2$$

$$- \frac{2}{EI\lambda} (L-D/\lambda)^2$$



DOUBLE CANTILEVER SANDWICH BEAM

Figure 1. Double cantilever sandwich beam with extensometer mounted for compliance measurements.

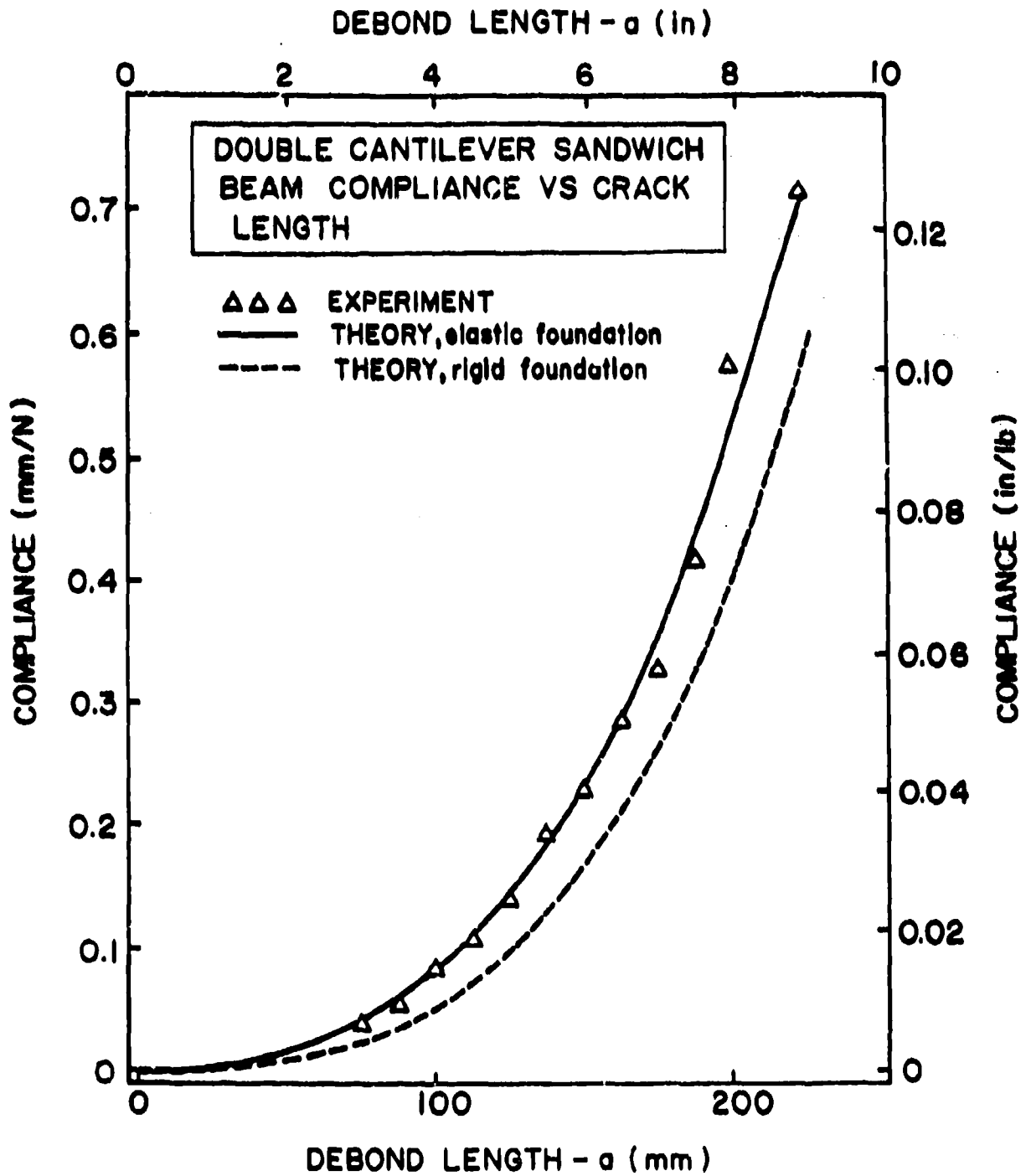
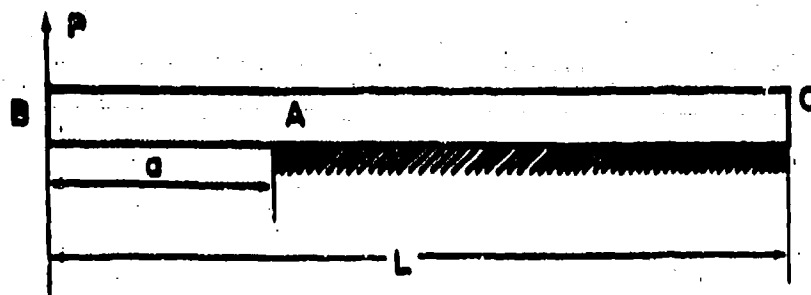


Figure 2. Experimental and predicted compliances as a function of debond distance (specimen #1).



FINITE BEAM ON ELASTIC FOUNDATION

Figure 3. Upper half of DCSB specimen modeled as a beam on an elastic foundation.

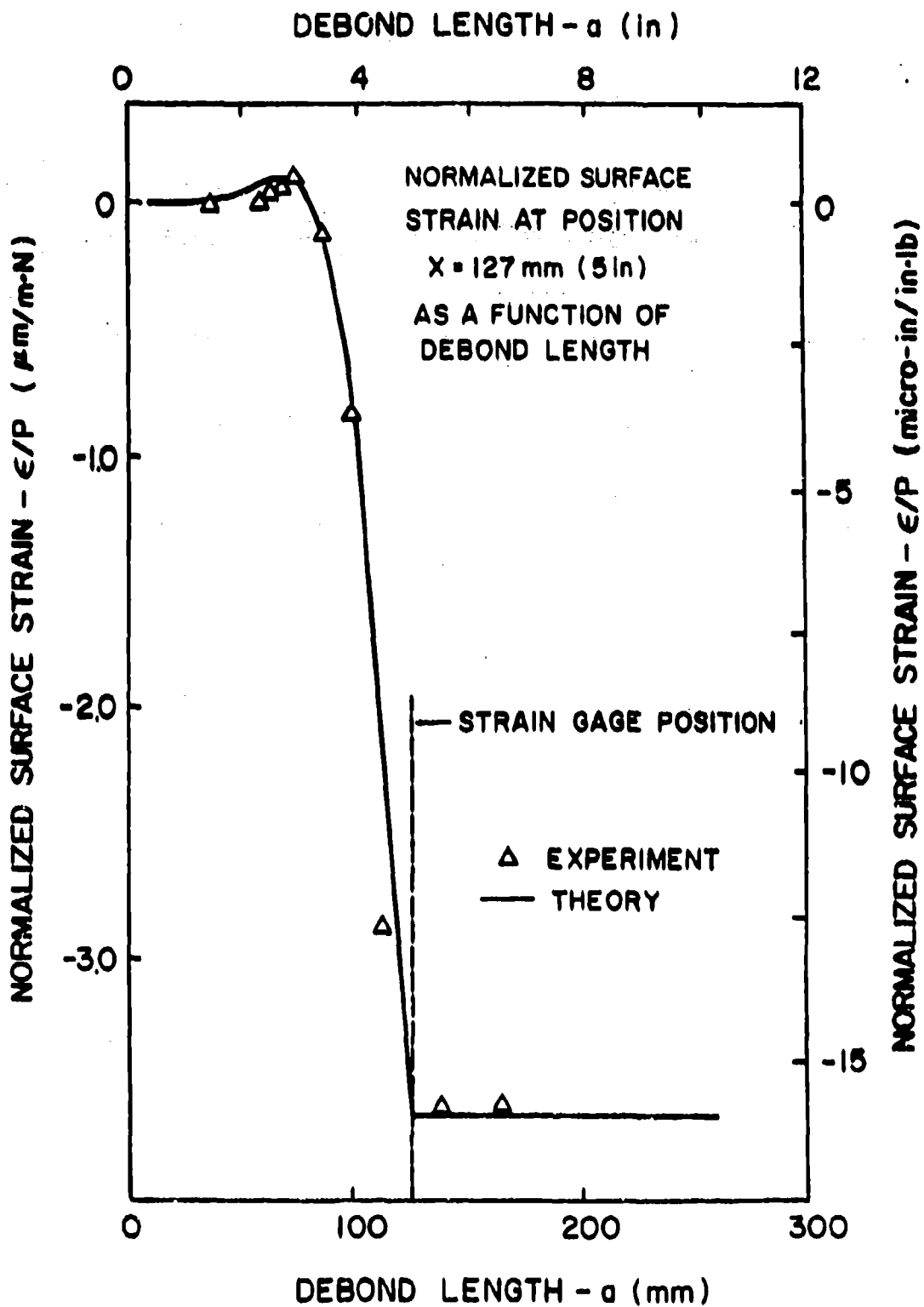


Figure 4. Comparison of experimental and predicted values of normalized surface strain at position $x = 127 \text{ mm}$ (5 in) as a function of debond length (specimen #2).

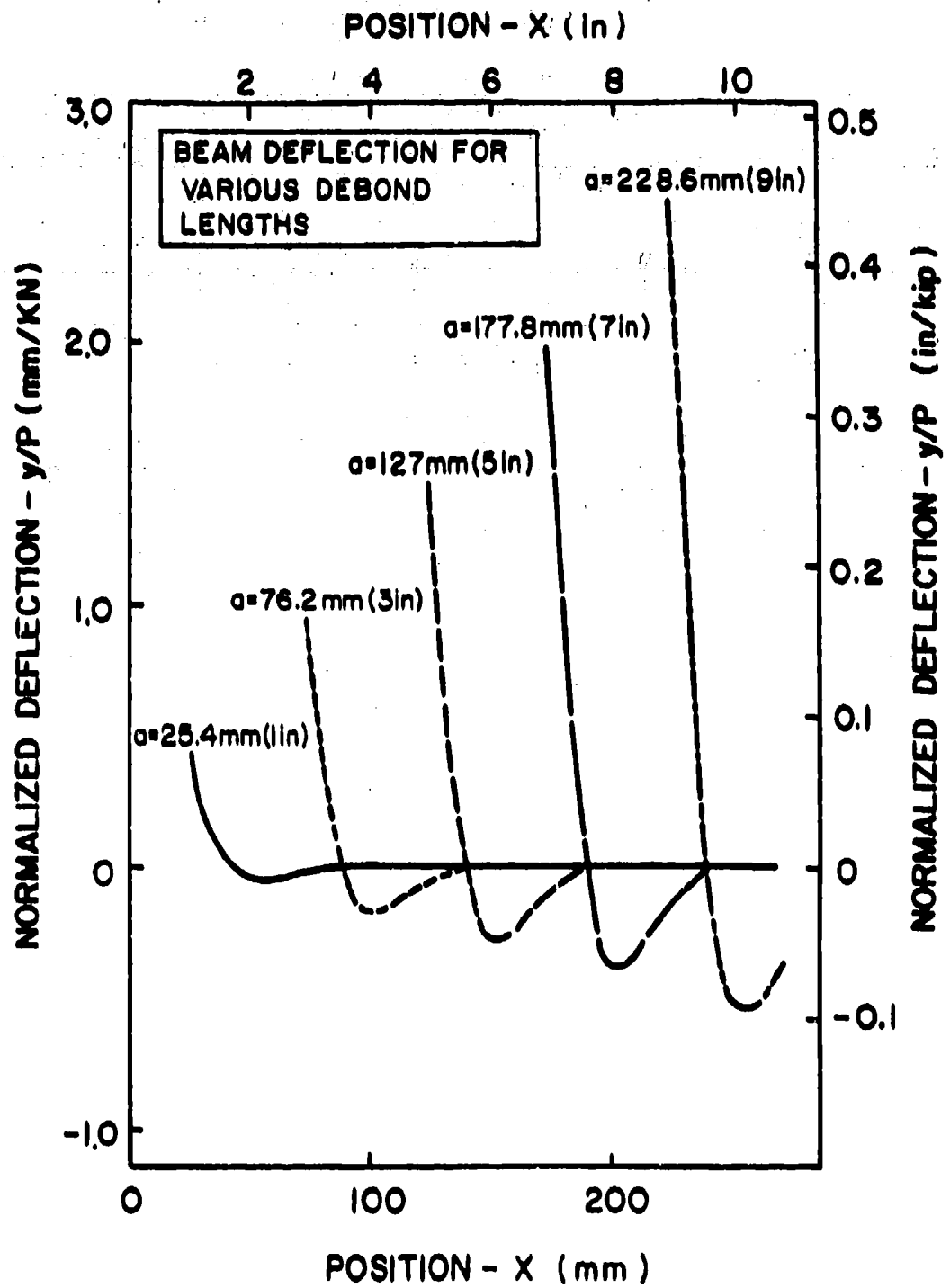


Figure 5. Analytical predictions of normalized deflections for different rubber layer thicknesses.

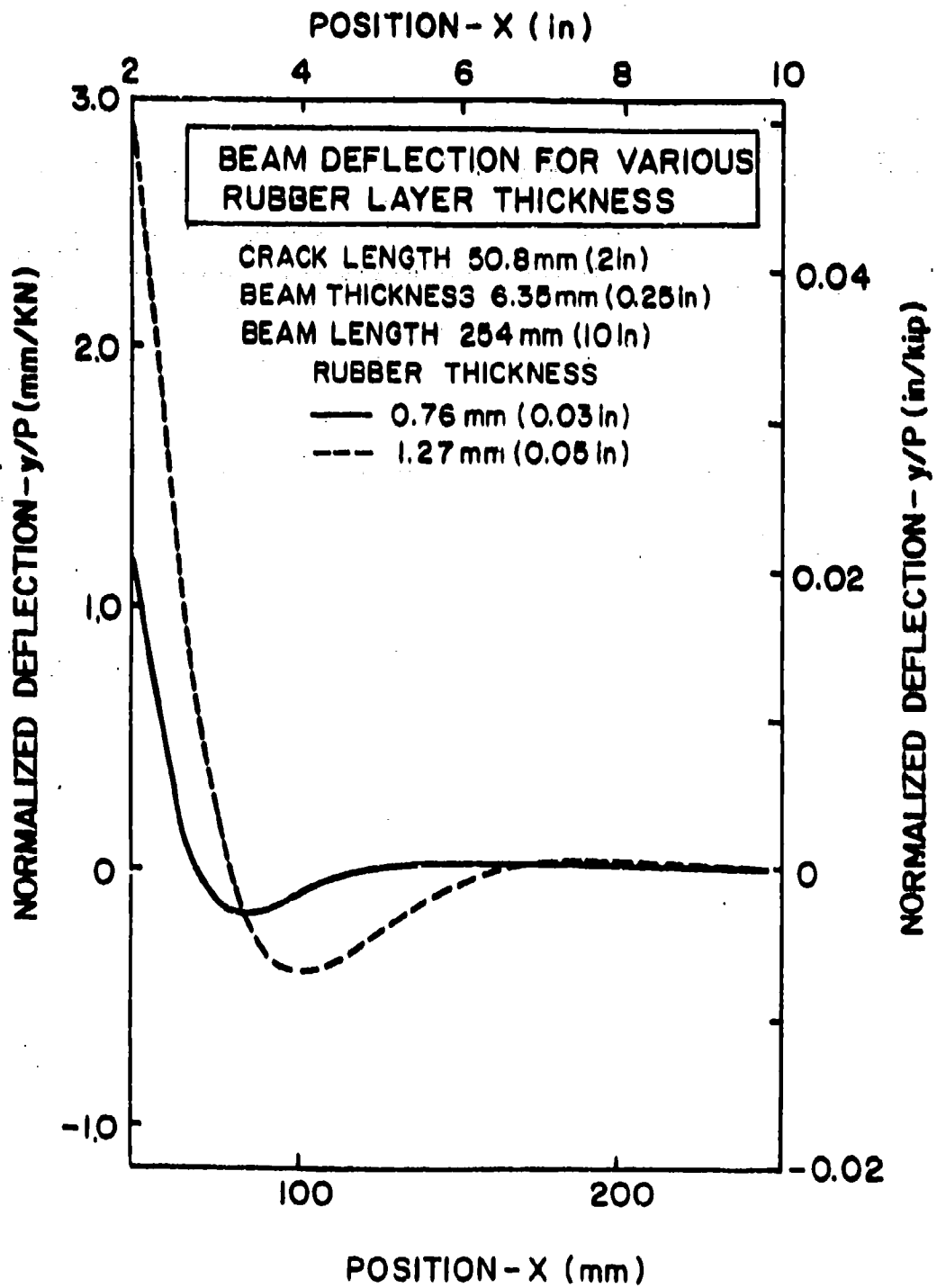


Figure 6. Predicted values of normalized deflections for different rubber layer thicknesses.

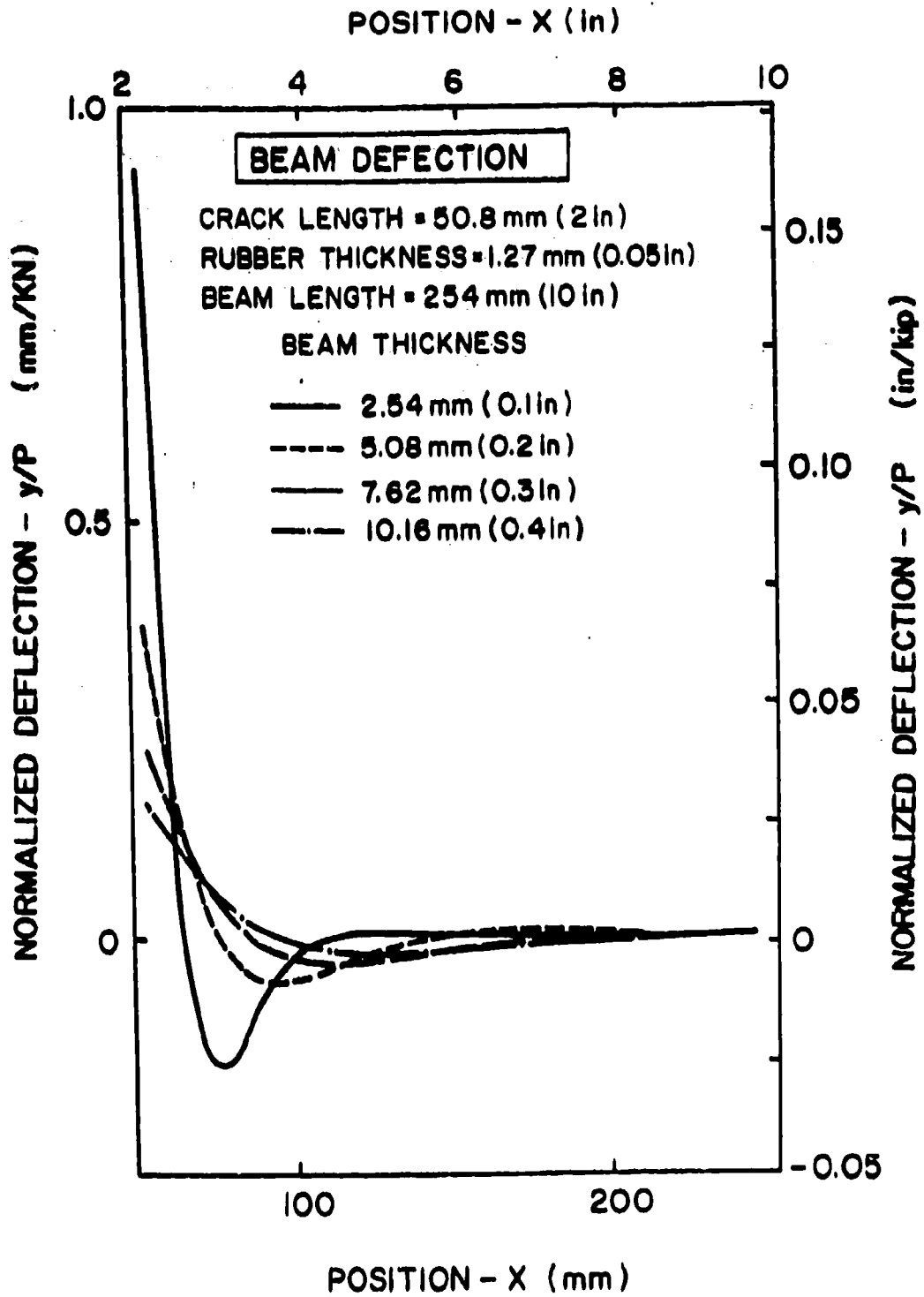


Figure 7. Predicted values of normalized deflection for several beam thicknesses.

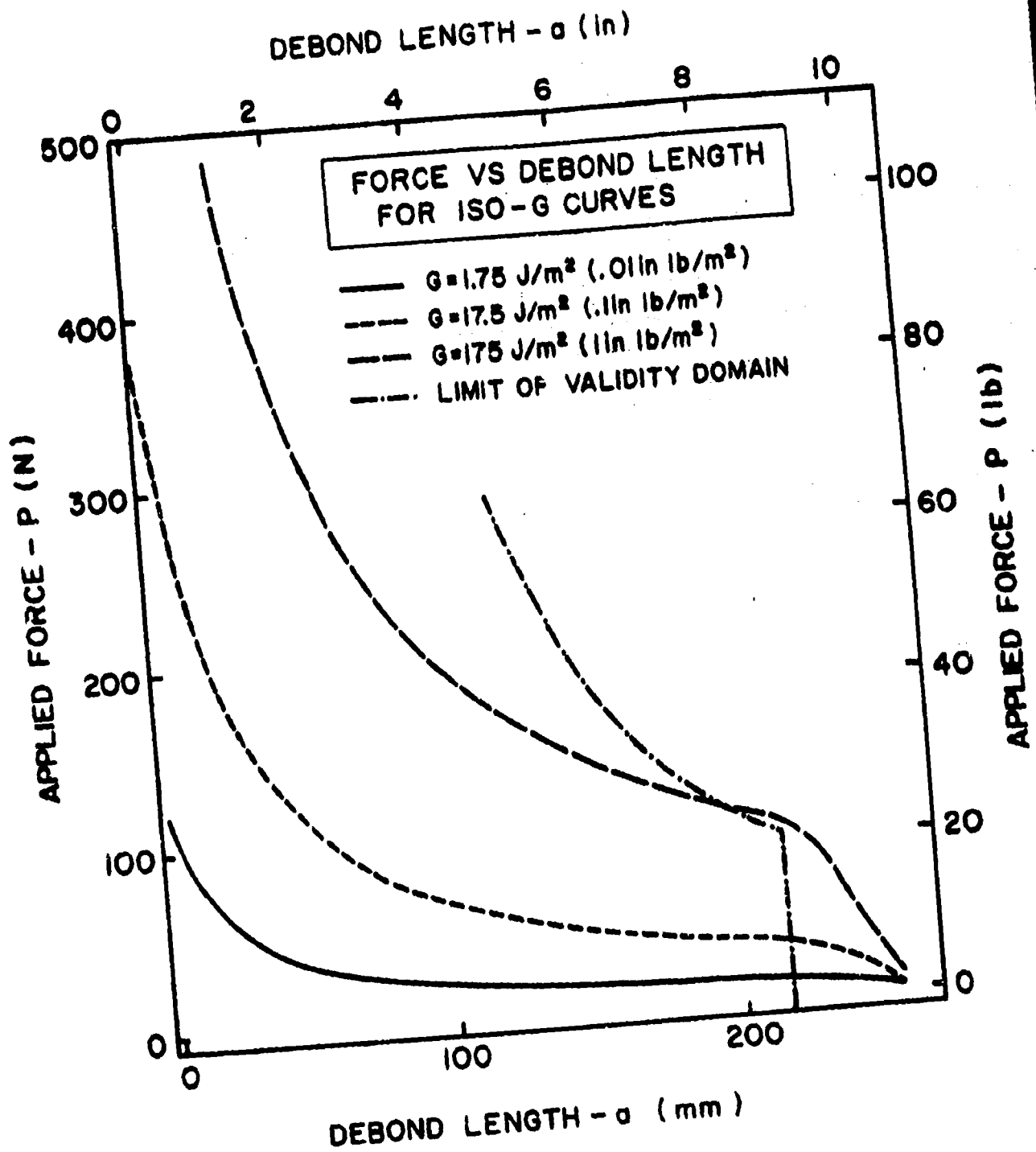


Figure 8. Analytical predictions of load decay as a function of crack length for several constant strain energy release rates, G (specimen #2).

EXPERIMENTAL SETUP FOR ACCELERATED CATHODIC DELAMINATION OF DOUBLE CANTILEVER SANDWICH BEAM

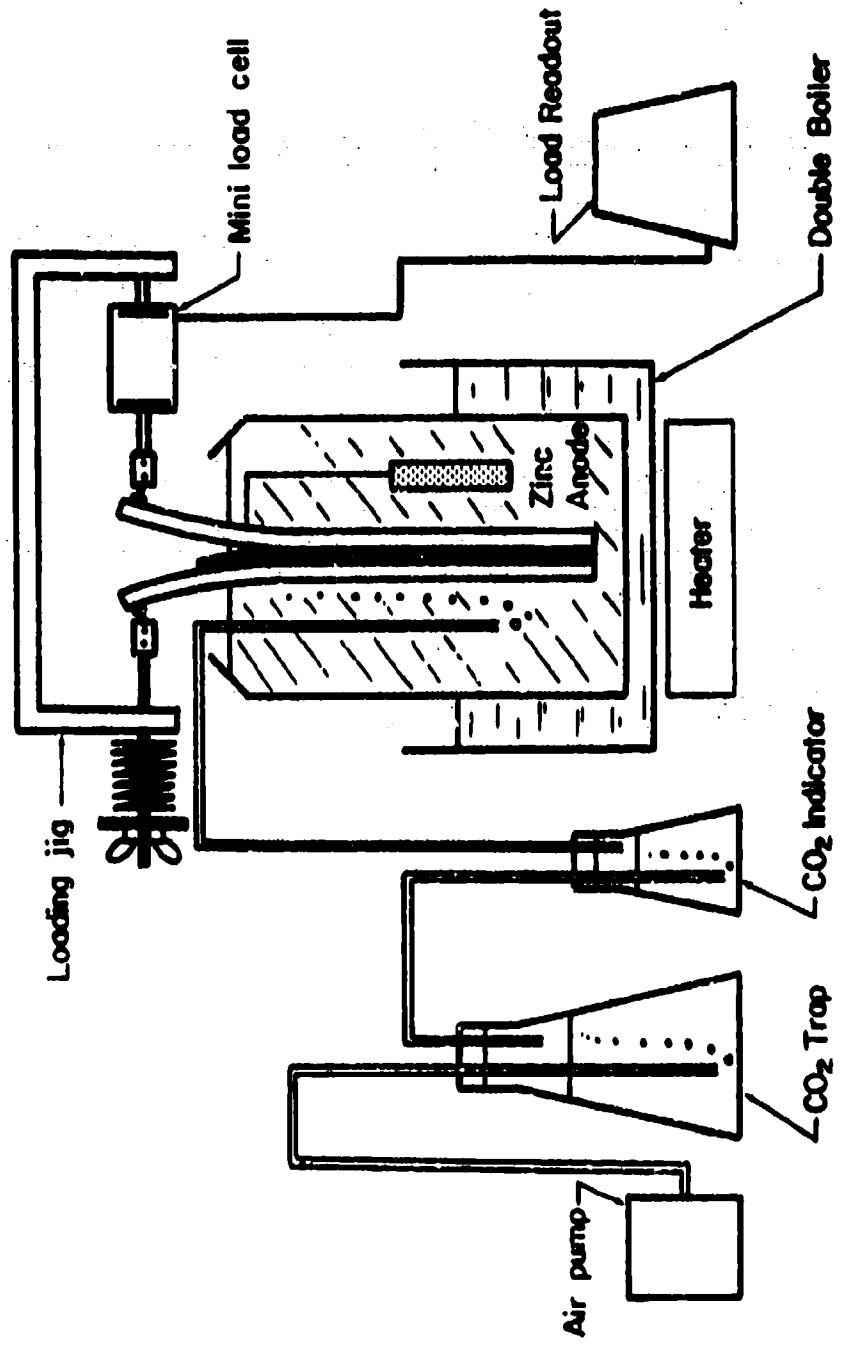


Figure 9. Experimental setup for accelerated cathodic delamination of a rubber-to-steel adhesive joint.

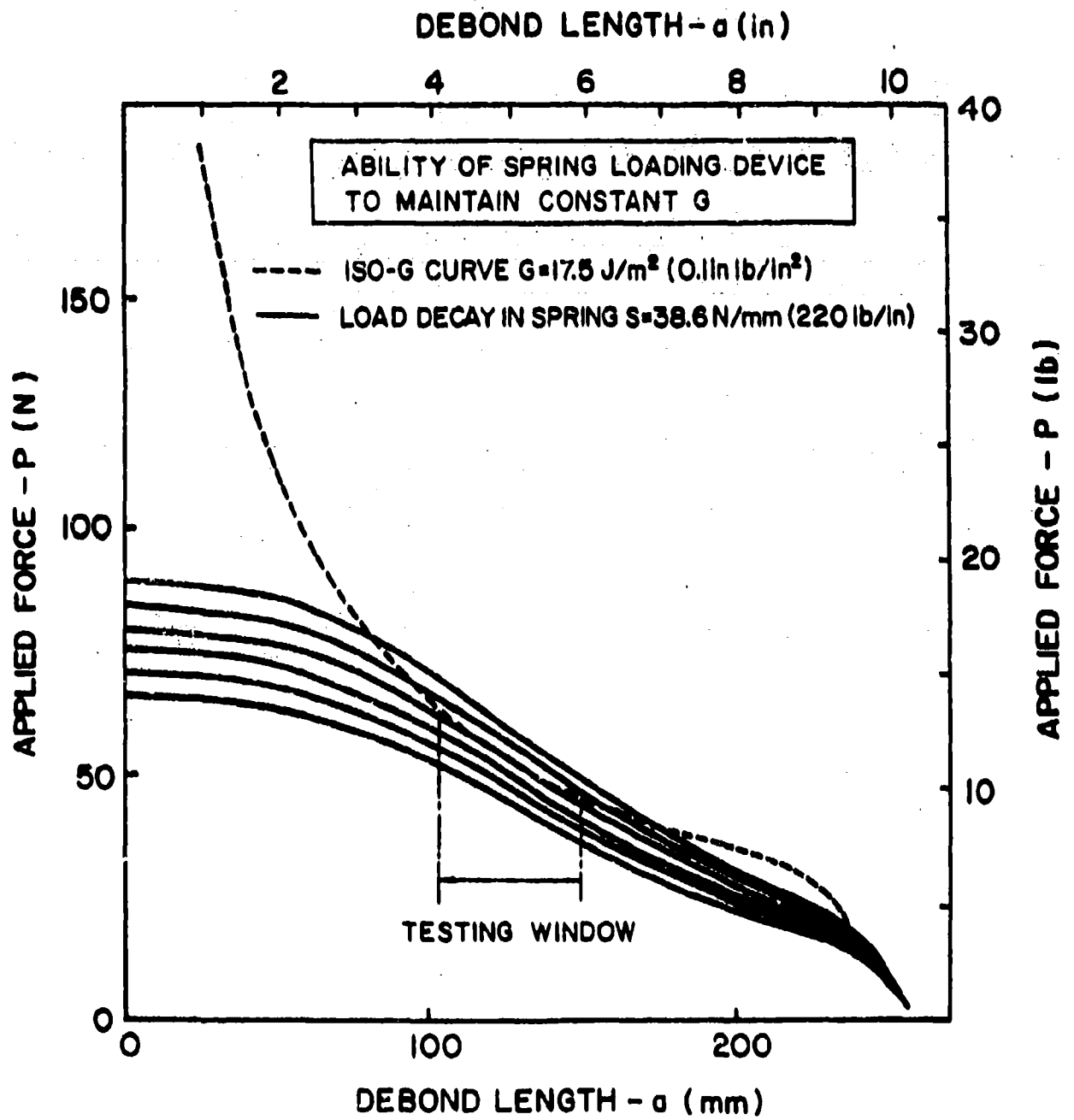


Figure 10. Available strain energy release rates for several spring preloads on an Iso-G curve.

4. Title and Subtitle The Development of a Modified Double Cantilever Beam Specimen for Measuring the Fracture Energy of Rubber to Metal Bonds		5. Report Date November 20, 1986
7. Author(s) Lefebvre, Didier R. and Dillard, David A.		8. Performing Organization Rept. No. CAS/ESM-86-3 VPI-E-86-26
9. Performing Organization Name and Address Virginia Polytechnic Institute & State University Center for Adhesion Science and Department of Engineering Science and Mechanics Blacksburg, VA 24061		10. Project/Task/Work Unit No.
12. Sponsoring Organization Name and Address Office of Naval Research 800 N. Quincy Street Arlington, VA 22217		11. Contract/Grant No. N00014-82-K-0185 P00005
		13. Type of Report & Period Covered Interim Report 4/85-4/86
		14.

15. Supplementary Notes
Prepared for publication

16. Abstracts
Rubber to metal bonds are important in a variety of automotive, tire and marine applications. A new technique is discussed for measuring the strain energy release rates of these adhesively bonded joints in the presence of harsh environments. Guidelines for design and applications are given.

17. Key Words and Document Analysis. 17a. Descriptors

17b. Identifiers/Open-Ended Terms

17c. COSATI Field/Group

18. Availability Statement Unlimited	19. Security Class (This Report) UNCLASSIFIED	21. No. of Pages 27
	20. Security Class (This Page) UNCLASSIFIED	22. Price